IMPROVEMENT OF WALL SURFACE TEMPERATURE EVALUATION PROCEDURE DURING SUBCOOLED NUCLEATE BOILING IN NON-EMPIRICAL BOILING AND CONDENSATION MODEL

Y. Ose*
Yamato System Engineer Co., Ltd.
1-17-1 Wakaba-cho, Hitachi, Ibaraki, 317-0063, Japan
ose@yse.co.jp

T. Kunugi
Department of Nuclear Engineering
Kyoto University
Kyoto-Daigaku Katsura, Nishikyo-Ku, Kyoto, 615-8540, Japan
kunugi@nucleng.kyoto-u.ac.jp

ABSTRACT

In order to predict the nucleate boiling bubble behavior and its heat transfer characteristics by means of a direct numerical simulation (DNS), a non-empirical boiling and condensation model was developed by the authors. This model was based on the quasi-thermal equilibrium hypothesis and consisted of an improved phase-change model and a relaxation time model. The MARS (Multi-interface Advection and Reconstruction Solver) combined with this model was performed for transient three dimensional DNSs on a single bubble behavior of the subcooled nucleate pool boiling. In this simulation, because of neglecting the microlayer underneath the bubble-base, the predicted bubble-departure-time period from its nucleation site at relatively low subcooled condition showed the overestimated tendency compared to the visualization experimental results. It was also found that the wall surface temperature predicted beneath the growing bubble was higher than that of the experimental results. In this study, in order to overcome that discrepancy, the evaluation procedure of the wall surface temperature during the subcooled nucleate boiling in the non-empirical boiling and condensation model has been improved. Especially, the heat balance through the wall surface during the bubble growth period in the model has been improved to consider the microlayer evaporation effects underneath the bubble-base without any artificial microlayer model. As a validation of this improved procedure, DNSs on the same as the experimental conditions have been performed for a single bubble behavior of the nucleate pool boiling under low subcooled condition, and the numerical results were compared to the experimental one. The evolutions of wall surface temperature during the bubble growth period show the fairy good agreement between the experiment and the numerical simulation. Moreover, a significant improvement of the prediction accuracy for the bubble-departure-time period from its nucleation site under low subcooled condition was achieved by the improvement of the procedure.

KEYWORDS
Light water reactors, Boiling and condensation model, Subcooled nucleate boiling, Wall surface temperature, Direct numerical simulation

1. INTRODUCTION

The understanding of boiling phenomena is extremely important for the thermal hydraulics design of light water nuclear reactors such as BWR (Boiling Water Reactor). However, the boiling phenomena are extremely complicated due to the phase change process and many physical processes are involved. It is known that the elucidation of essential mechanism on the boiling phenomena is the most difficult and challenging issue. Since the boiling heat transfer has most distinguished efficiency, numerous experimentally and analytically studies have been carried out to clarify the boiling heat transfer characteristics. Recently, owing to a direct numerical simulation (DNS) is expected to be another promising approach to clarify the boiling phenomena, the numerical simulations for directly treating the bubble dynamics and heat transfer characteristics regarding the nucleate boiling have been performed by several investigators [1-10]. The review of latest direct numerical simulation on boiling phenomena has been reported by one of the authors [11].

In this situation, we developed a non-empirical boiling and condensation model to predict the nucleate boiling bubble behavior and its heat transfer characteristics by mean of DNS [12]. This model was based on the quasi-thermal equilibrium hypothesis and consisted of the following models: (1) an improved phase-change model based on the enthalpy method applying to the zero-thickness water-vapor interface and (2) introducing a relaxation time considering the unsteady heat conduction in the finite water-vapor interface. So far, by using the MARS (Multi-interface Advection and Reconstruction Solver) [13] combined with this model, we performed transient three dimensional direct numerical simulations for a single boiling bubble behavior starting the bubble growth from a pre-existed embryo, the bubble departure from the heating surface and finally the bubble shrinking behavior due to its condensation in the subcooled pool [12-15]. DNSs were conducted in same conditions of the visualization experiments as the validation data. The DNS results obtained regarding the bubble volume during the bubble growing and shrinking processes and the bubble shape during the bubble departure from the heating surface were agreed very well with the results of visualization experiments and the results of the existing analytical equations such as the Rayleigh equation in the inertia-controlled bubble growth process and the Plesset-Zwick equation in the heat-transfer controlled bubble growth process. The effects of the surface wettability for the bubble departing behavior were also investigated by using the DNS [16]. It was found that the predicted bubble-departure-time period from its nucleation site at relatively low subcooled condition, which is less than about 5 °C, showed the overestimated tendency compared to the visualization results, while the predicted bubble-departure-time periods with increasing of the degree of subcooling were well coincident with the visualization results [15]. This reason might be considered that the microlayer was neglected in this simulation, i.e., perfectly dry-out condition, so that, especially in the low subcooled condition which is close to the saturated boiling, it should be considered the effects of microlayer evaporation. On the other hands, the systematic study of comparison between the state-of-the-art experimental measuring data and the numerical simulations using MARS including this non-empirical boiling and condensation model has been conducted [17]. This experimental method was consisted of three measurements: the temporally synchronize and spatially map surface temperature distribution using an infrared thermometry, the liquid-vapor phase distribution using a total reflection technique, and the microlayer geometry using a laser interferometry. As a result, it was found that the heating surface temperature beneath the growing bubble at the beginning of bubble growth obtained from the numerical simulations was higher compared to that of the experimental results. It can be considered that the amount of heat removal from the heating surface due to the phase change tends to be under-predicted in these simulations.

This paper described that the evaluation procedure of the wall surface temperature during the subcooled nucleate boiling in the non-empirical boiling and condensation model was improved to establish more accurate prediction model for the boiling heat transfer. At first, two-dimensional axisymmetric DNS of a single bubble nucleate boiling based on the MARS with non-empirical boiling and condensation model

was performed. The conditions of numerical simulations were similar to that of the experiments [17]. In order to consider the microlayer evaporation effects without a microlayer model, the heat balance through the wall surface during the bubble growth period was improved. Using this improved procedure, transient three-dimensional DNS of the single bubble departure behavior at low subcooled condition similar to the previous study [15] was performed to examine the prediction accuracy of the bubble-departure-time period.

2. NUMERICAL METHOD

2.1. Governing equations of MARS

The governing equations of the MARS are consisted of the continuity equation for multi-phase flows, the momentum equation based on a one-fluid model and the energy equation with an external work done by a phase-change phenomenon as follows:

$$\frac{\partial F_m}{\partial t} + \nabla\left(F_m \mathbf{u}\right) - F_m \nabla \mathbf{u} = 0 \tag{1}$$

$$\frac{\partial \mathbf{u}}{\partial t} + \nabla \cdot \left(\mathbf{u}\mathbf{u}\right) = \mathbf{G} - \frac{1}{\langle \rho \rangle}\left(\nabla P - \nabla \cdot \boldsymbol{\tau} + \mathbf{F}_v\right) \tag{2}$$

$$\frac{\partial}{\partial t}\langle \rho C_v \rangle T + \nabla \cdot \left(\langle \rho C_v \rangle T \mathbf{u}\right) = \nabla \cdot \left(\langle \lambda \rangle \nabla T\right) - P\left(\nabla \cdot \mathbf{u}\right) + Q \tag{3}$$

where F is volume of fluid (VOF) fraction, the suffix m denotes the m-th fluid or phase, $\mathbf{u}$ is velocity, t time, P pressure, T temperature, $\mathbf{G}$ gravity, $\boldsymbol{\tau}$ viscous shear stress, $\mathbf{F}_v$ body force due to a surface tension and a wall adhesion based on the continuum surface force (CSF) model [18], ρ density for each phase, $\bar{\rho}$ a half density between water and vapor, C_v specific heat at constant volume, λ thermal conductivity, Q heat source and a bracket < > denotes an average of thermal properties. In order to satisfy the conservation of F, the third term of the continuity equation (Eq. (1)) must be included. The second term of the right hand side of the energy equation (Eq. (3)), i.e., the Clausius-Clapeyron relation was considered as the external work done by a phase change. Moreover, a bubble oscillation caused by the expansion and contraction with the bubble growth and condensation processes was also modeled to reduce the limitation of the incompressible fluid assumption. The interface volume-tracking technique [13] was applied to the continuity equation in the MARS. The projection method [19] was applied to solve the momentum equation and the pressure Poisson equation was solved by the Bi-CGSTAB [20].

2.2. Non-empirical boiling and condensation model

2.2.1. Improved phase-change model

The Non-empirical boiling and condensation model for the subcooled nucleate boiling phenomena consisted of the improved phase-change model and the relaxation time model based on the quasi-thermal equilibrium hypothesis [12]. The improved phase-change model is based on the temperature-recovery method [21]. Since the temperature-recovery method could not treat a large volume change in the expansion and condensation process because this method was originally developed for solidification/melting of metals, the improved phase-change model was considered a large volume change between water and vapor. This model was applied only to the interfacial cell which has the VOF fraction between 0 and 1, and its procedure is as follows:

1) Temperature distribution in the whole solution domain is calculated by solving the energy equation (Eq.(3)) without the phase-change.
2) The following a phase-change ratio Δg_v considering the density-change between water and vapor is computed.

$$\Delta g_v = \frac{\rho_l c_{pl} \Delta T}{\rho_g h_{lv}} \tag{4}$$

where, c_{pl} is specific heat at constant pressure, ΔT temperature difference from the saturation temperature (T_{sat}-T), h_{lv} latent heat of vaporization and the suffixes of g and l denote gas and liquid phases, respectively.

3) The temperature in the interface cell which done with phase-change recovers to T_{sat}.
4) Finally, the following constraint condition is satisfied to conserve the total volume.

$$\left(F_l - |\Delta g_v|\right) + \left(F_g + |\Delta g_v|\right) = 1 \text{ : At evaporation} \tag{5}$$

$$\left(F_l + |\Delta g_v|\right) + \left(F_g - |\Delta g_v|\right) = 1 \text{ : At condensation} \tag{6}$$

2.2.2. Relaxation time model

The improved phase-change model consists of Eps. (4)–(6) based on the assumptions of both a zero-thickness interface and a "rapid" phase-change from "State 1 (Water)" to "State 2 (Vapor)" or *vice versa* due to the local quasi-thermal equilibrium hypothesis. This hypothesis requests another contradictory assumption that is a "very slow" phase-change from "State 1" to "State 2". In order to satisfy this requirement, a finite thickness of interface must be considered and both from/to "very slow" to/from "rapid" changes will occur simultaneously in the phase-change process. This process can be described by a relaxation or waiting time for consuming the latent heat at the interface region i.e., the unsteady heat conduction in the finite interface region as the "very slow" change process: The relaxation time t_Δ can be defined as a time that the phase-change front is passing through a fictitious interface thickness Δ, so that t_Δ can be expressed by using the thermal diffusivity of the water α as follows:

$$t_\Delta = \frac{\Delta^2}{\alpha} \tag{7}$$

On the other hand, a well-known thermal penetration length δ for the unsteady heat conduction in a semi-infinite slab with a constant boundary temperature was approximated by the following expression:

$$\delta = \sqrt{12 \alpha t} \tag{8}$$

If the thermal penetration depth can be assumed as the same as the fictitious interface thickness, t_Δ can substitute into Eq. (8):

$$\delta = \sqrt{12} \Delta \tag{9}$$

As the result, an invariant relation between the thermal penetration length and the fictitious interface thickness can be obtained as follows:

$$\frac{\Delta}{\delta} = \frac{1}{\sqrt{12}} \approx 0.3 \tag{10}$$

According this relationship, the fictitious interface thickness in around 30% of the thermal penetration depth corresponds to the "very slow" phase-change process. In other words, the rapid phase-changed volume during t_{Δ} is 70% of the thermal penetration depth, not 100%. In this study, the relaxation time can be considered to control the VOF fraction as a phase-change limiter. For example, the relaxation time for both phase-fronts is assumed to be 15% at either of the interface, such as evaporation or condensation front:

$$\text{VOF limiter: } 0.15 \le F \le 0.85 \tag{11}$$

3. NUMERICAL SIMULATION

3.1. Computational Domain and Conditions

In order to validate the prediction accuracy of the wall surface temperature during the nucleate boiling for the non-empirical boiling and condensation model, a two-dimensional axisymmetric numerical simulation of a single bubble nucleate boiling has been performed. The conditions for the numerical simulation were taken from [17]. Figure 1 shows the two-dimensional axisymmetric computational domain in this simulation. Although the numerical simulations under the two-dimensional Cartesian coordinate system were conducted in [17], in this study, the two-dimensional cylindrical, *r*-*z* coordinate system was used for the computational domain to assume the axisymmetric bubble growth. The computational domain was of dimensions 7.5×10 mm in radial distance (*r*) and height (*z*), respectively. The grid size was 50 μm in both *r*- and *z*- directions. The numbers of cells was 150×200 in *r*- and *z*- directions, respectively. The time step in the computation was set to less than 10 μs to satisfy the Courant number kept 0.1. The working fluid was water at a system pressure of 101.3 kPa, and the degree of subcooling in the water was 3°C. The boundary conditions at right (*r*+) and bottom (*z*-) sides of the computational domain were the slip-wall with adiabatic condition. The Dirichlet boundary conditions of both pressure of 101.3 kPa and temperature of 97.0 °C were imposed at the top (*z*+) side of the computational domain. The heater of 50μm in thickness used in the experiment was located on the CaF_2 base plate of 0.75mm in thickness at the bottom of computational domain, which supplies the input volumetric heat source of 1.09 GW/m^3 corresponding to the heat flux on the heating surface in the experiment: 53 kW/m^2. The initial wall surface temperature was set to 120 °C corresponding to a bubble nucleation temperature on the wall surface from the experiment. The solid heat conduction from the heater surface to CaF_2 base plate was numerically considered. The static contact angle between the liquid and the surface was taken to be 15° less than that of experiment of 65° as the same condition of [17], for which the effect of dynamic contact angle was not considered in this simulation. The setting of initial temperature field in the thermal boundary layer on the wall surface plays a significant role in the bubble growth behavior for nucleate boiling. However, the temperature field surrounding the layer remains unknown in the experiment. Therefore, the unsteady heat conduction computation in the whole solution domain was conducted until the surface temperature reaches 120 °C to form the initial thermal boundary layer in this simulation. After that, the initial vapor bubble as a hemispherical shape of 100 μm in radius, which was assumed to be the saturated temperature under the atmospheric pressure, was put the center of *r*-direction on the wall surface. The initial velocity field in this simulation was assumed to be zero.

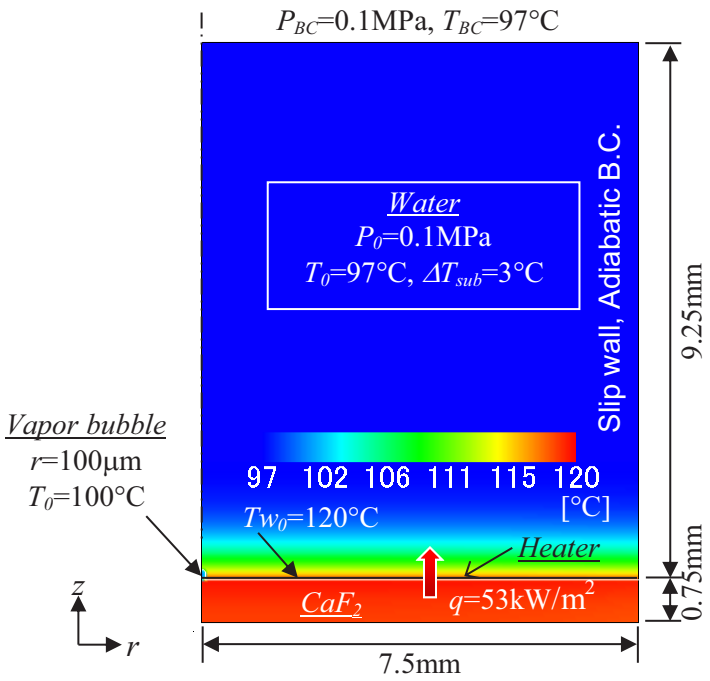

Figure 1. Computational domain.

3.2. Results and discussions

Figure 2 shows the time evolution results of the numerical simulation for the single bubble nucleate boiling of water in the degree of subcooling 3 °C. The results show that the liquid-vapor interface of the white line which corresponded the VOF fraction of 0.5, the temperature distribution as shown by the color contour in the range from 111°C to 121°C, and the velocity vectors. It can be seen that the initial vapor bubble grows rapidly in the superheated liquid layer, and the wall surface underneath the bubble-base became a dry-out area immediately, because the microlayer was neglected in this simulation. On the other hands, with growth of the bubble on the surface in the water, the surface temperature of the dry-out region inside the triple (solid-liquid-vapor) contact line underneath the bubble-base increases rapidly, while the surface temperature near the triple contact line gradually decreases. In fact, this tendency shows a result similar to that of the numerical simulation based on the MARS using the non-empirical boiling and condensation model [17]. Eventually, the vapor bubble did not depart from the heating surface in this simulation due to the high surface temperature of dry-out region. However, according to the experimental result [17], the drops of local surface temperature about 5 °C underneath the babble-base and 10 °C at the triple contact line were observed until the bubble departing from the surface. With regard to this discrepancy of temperature characteristics underneath the bubble-base on the boiling surface, we must consider the well-known effect of the microlayer evaporation there without any artificial microlayer model.

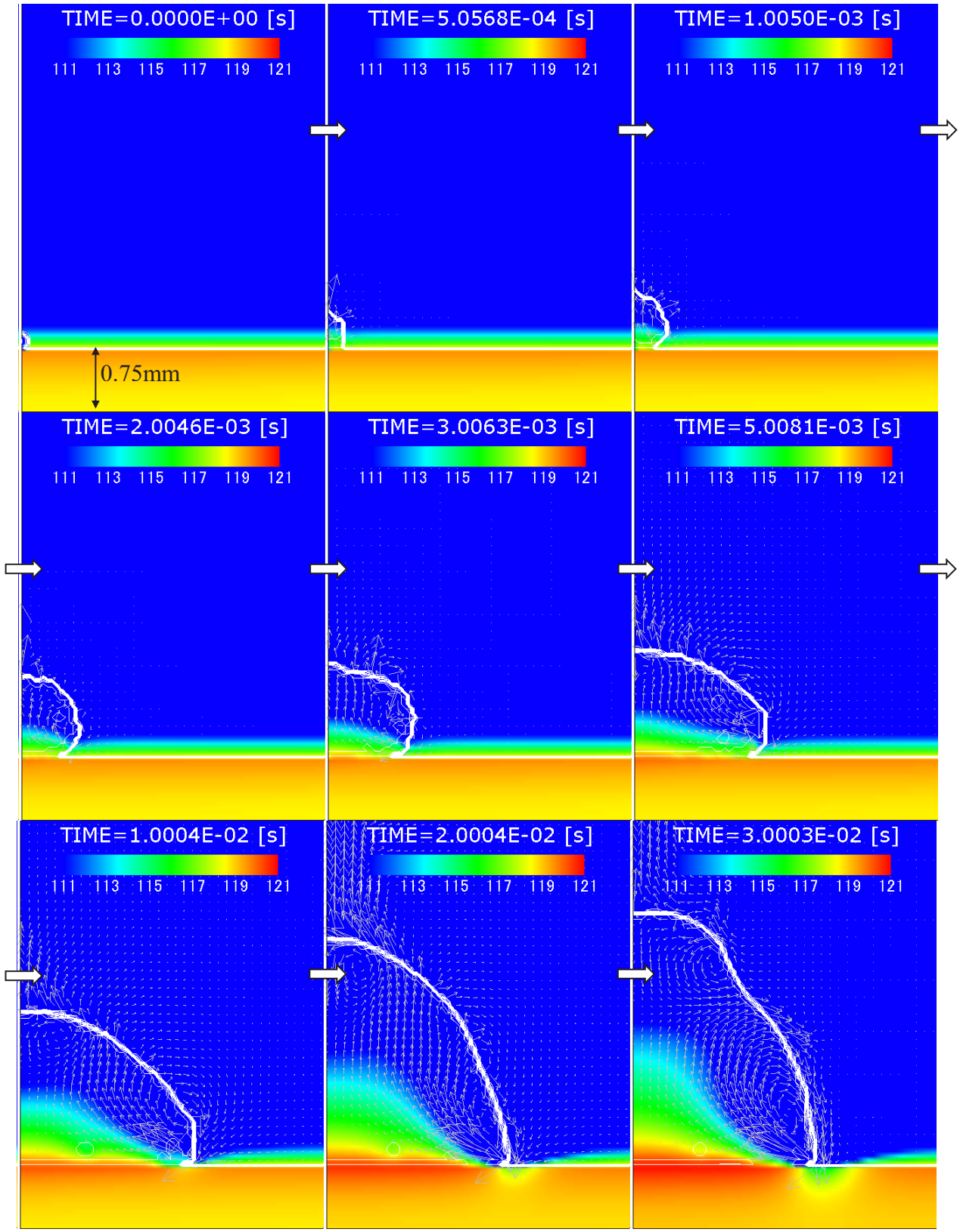

Figure 2. Numerical results of bubble shape, temperature distribution and velocity vector using previous procedure [15].

Although it seems that the microlayer plays a role in determining the evolution of surface temperature underneath the boiling bubble-base, the mechanism of microlayer has not yet been fully understood. Since the thickness of microlayer is usually assumed to be a few microns, the numerical simulation considering the microlayer requires tremendously small grid size such as a nano-scale and huge computational cost.

3.3. Improvement of Wall Surface Temperature Evaluation Procedure

As for the previous studies on the numerical simulation with the microlayer for nucleate boiling, a special wall boundary treatment has been proposed by Son et al. [3], Kunkelmann and Stephan [8, 9], Sato and Ničeno [10]. The special wall boundary treatment was called a micro-region model to introduce an artificial microlayer, and coupled to Navier-Stokes solvers. The model has several limitations: the value of the dispersion constant (the Hamaker constant) is unclear; steady-state conditions are assumed in the two-dimensional system; and a contact angle larger than 90° cannot be treated. In this study, since the development of an improved micro-region model is not currently our target, the wall surface temperature evaluation procedure during the nucleate boiling has been improved without an artificial model. Since this problem is a conjugate heat transfer problem between solid and fluid, the following procedure is applied to the determination of the surface temperature:

The heat flux to the wall surface, s of the heat conduction term in the energy equation was defined as follows:

$$q_s = -\lambda_s \frac{T_s - T_w}{\Delta x_{s,w}} = -\lambda_s \frac{T_f - T_s}{\Delta x_{s,f}} \tag{12}$$

where, q is heat flux, λ thermal conductivity, T temperature and Δx_s distance to the wall surface. The subscripts w and f denote the wall and fluid computational cells adjacent to the wall surface, respectively. Figure 3 shows the definition of variable location in Eq. (12) at the wall surface between the fluid and wall cells. The circle symbols in Fig. 3 are the definition point in the fluid and wall computational cells. The thermal conductivity at the wall surface, λ_s in Eq. (12) can be defined by using a harmonic average between the fluid, f and wall, w cells as follows:

$$\lambda_s = \frac{\Delta x_{s,f} + \Delta x_{s,w}}{\left(\frac{\Delta x_{s,f}}{\lambda_f} + \frac{\Delta x_{s,w}}{\lambda_w} \right)} \ , \ \lambda_f = F_g \lambda_g + F_l \lambda_l \tag{13}$$

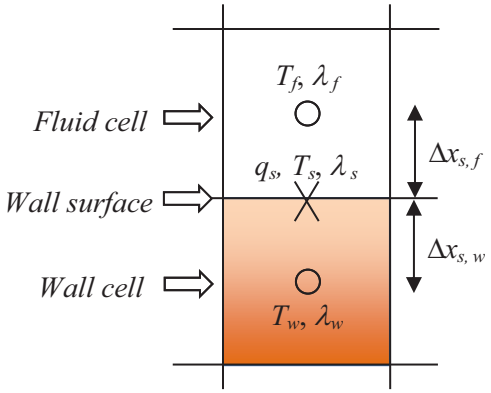

Figure 3. Definition of variable location at wall surface between fluid and wall cells.

It seems that the thermal conductivity at the wall surface, λ_s in Eq. (12) is a rational definition, if the fluid cell has not been the phase-change process. However, when the microlayer evaporation on the wall surface underneath the growing bubble-base occurs under the fluid cell, the definition of thermal conductivity at the wall surface, λ_s could not be applied the harmonic average between the fluid and wall cells, because the thermal conductivity of fluid cell, λ_f adjacent to the wall surface during the bubble growth period in this simulation could be evaluated that of the almost gas phase due to the thinness of microlayer. Therefore, it could be considered that the heat removal from the wall surface causes the under-estimation in this simulation. Since the temperature of microlayer, T_{mlayer} on the wall surface can be assumed to be the saturated temperature, T_{sat} corresponding to its pressure by the improved phase-change model and of course the thickness is very thin, it can be considered that the surface temperature, T_s approaches the temperature of microlayer, T_{mlayer} during the phase-change process, i.e., the saturated temperature, T_{sat}. Assuming that the microlayer on the wall surface underneath the bubble-base exists during the bubble growth period in this simulation, a certain kind of the internal temperature boundary condition at the wall surface considering the effect of microlayer evaporation during the bubble growth period could be necessary to Eq. (12). Therefore, the heat balance at the microlayer surface between the wall and fluid cells assuming the microlayer evaporation has been improved as follows:

$$q_s = -\lambda_w \frac{T_{mlayer} - T_w}{\Delta x_{s,w}} = -\lambda_f \frac{T_f - T_{mlayer}}{\Delta x_{s,f}} \tag{14}$$

In Eq. (14), the thermal conductivity at the wall surface, λ_s is replaced by that of wall cell, λ_w or fluid cell, λ_f from Eq. (12), because the internal temperature boundary condition at the wall surface is applied. The temperature of microlayer surface, T_{mlayer} is used for the temperature gradient to the wall or the fluid cell in Eq. (14) to consider the effects of microlayer evaporation, instead of the surface temperature, T_s.

Figure 4 shows the time evolution of the bubble shape, the temperature distribution and velocity vector obtained from the numerical simulation using the improved procedure, in the same way as shown in Fig. 2. It can be seen that the drops of the local surface temperature of dry-out region underneath the bubble-base during the bubble growth period appears, owing to the consideration of the heat removal effects of microlayer evaporation presented by this procedure. It seems that the surface temperature decreases even more rapidly at the triple contact line than the dry-out region. These tendencies are in qualitatively agreement with the experimental results without any artificial microlayer model for microlayer in this simulation.

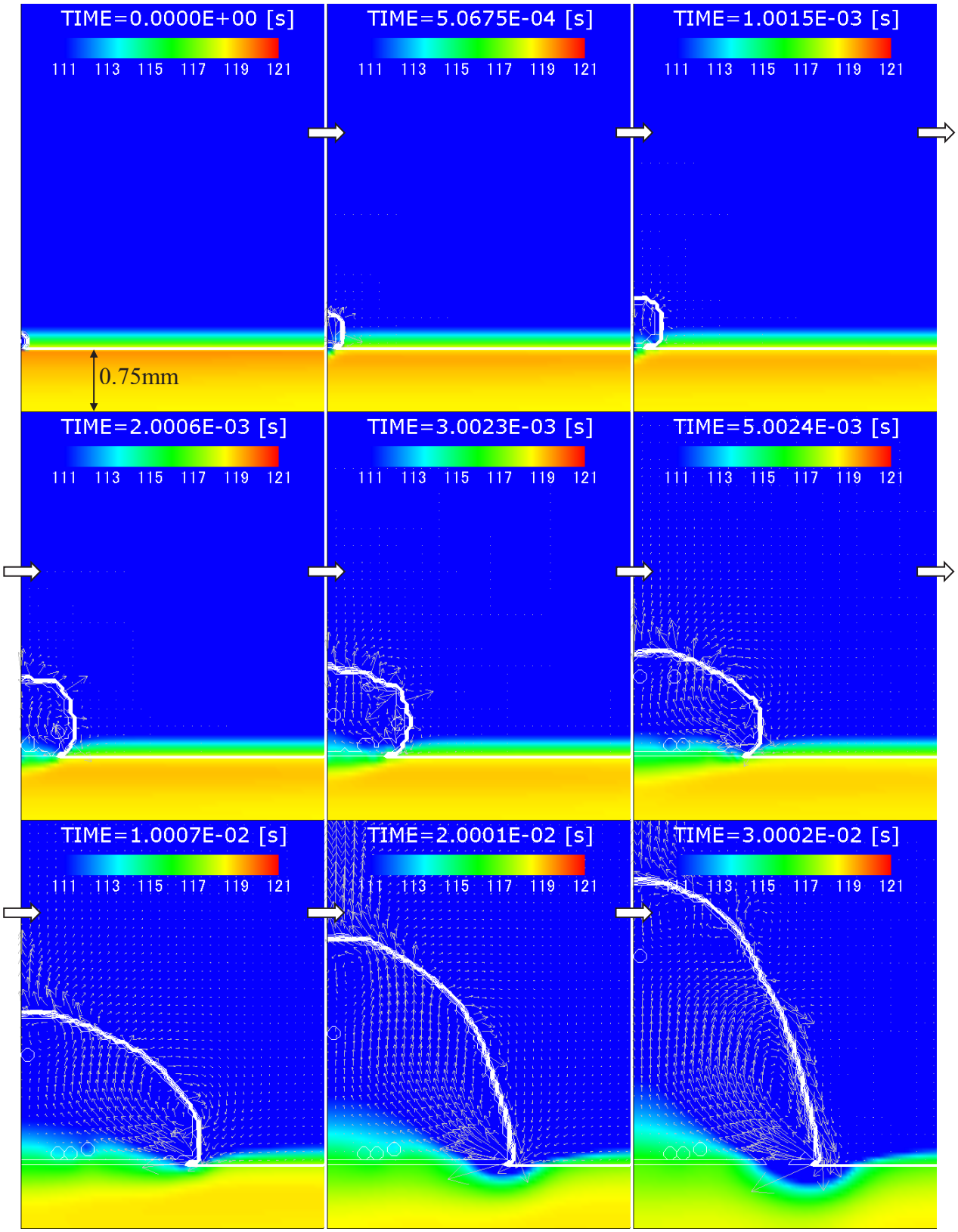

Figure 4. Numerical results of bubble shape, temperature distribution and velocity vector using improved procedure.

3.4. Application to Single Bubble Departure Simulation in Subcooled Pool Boiling

The improved procedure as mentioned previous section has been applied to the unsteady three-dimensional numerical simulation of a single bubble departure behavior from the heating surface during the nucleate pool boiling to validate the prediction accurately of the bubble-departure-time period from its nucleation site at relatively low subcooled condition. The numerical simulation was conducted as the same conditions of visualization experiments under atmospheric pressure by Kawara et al [22] and previous simulation by the authors [15]. The detail description of computational domain and conditions in this simulation are described in the reference [15]. The degree of subcooling in the water was set to 5 °C in this simulation, whose condition was shown the overestimated bubble-departure-time period by using the previous procedure compared to that of experiments. The initial bubble size was set to 0.62 mm and 0.47 mm in major- and minor-radius as a spheroid shape, which was assumed at the maximum bubble size in a horizontal direction obtained from the experimental data, since this simulation focuses on the bubble departure behavior from the heating surface after the bubble growth process. The temperature and velocity fields after one bubble departure were used as the initial field condition in this simulation.

Figure 5 shows the comparison of the time variation of bubble aspect ratio between height H and width W of the bubble until the bubble departure from the heating surface, between the experimental results and numerical one which were obtained by using both the previous procedure and improved one. In Fig. 5, the symbol denotes the experimental results. The numerical results obtained by using both the previous procedure and improved one are presented in the black and pink lines, respectively. When the bubble aspect ratio is less than 1.0, the bubble shape shows a flattened one, whereas the bubble shape shows a vertically-elongated one when the bubble aspect ratio is greater than 1.0. It can be seen that the evolution of bubble aspect ratio predicted by the numerical simulations using the improved procedure as well as that using the previous procedure were found to be in very good agreement with the experimental result. On the other hands, as for the time-departure-time period, t_D, although it can be seen the discrepancy between the numerical result using the previous procedure and the experimental result, the numerical results using the improved procedure is in fairly good agreement with the experimental result, because of the accurately estimated the surface temperature underneath the bubble-base. As the result, it was revealed that the improved procedure is predictably effective against the improvement of prediction accuracy of the time-departure-time period at low subcooled condition as well as the surface temperature underneath the bubble-base during the bubble growth period in the nucleated boiling.

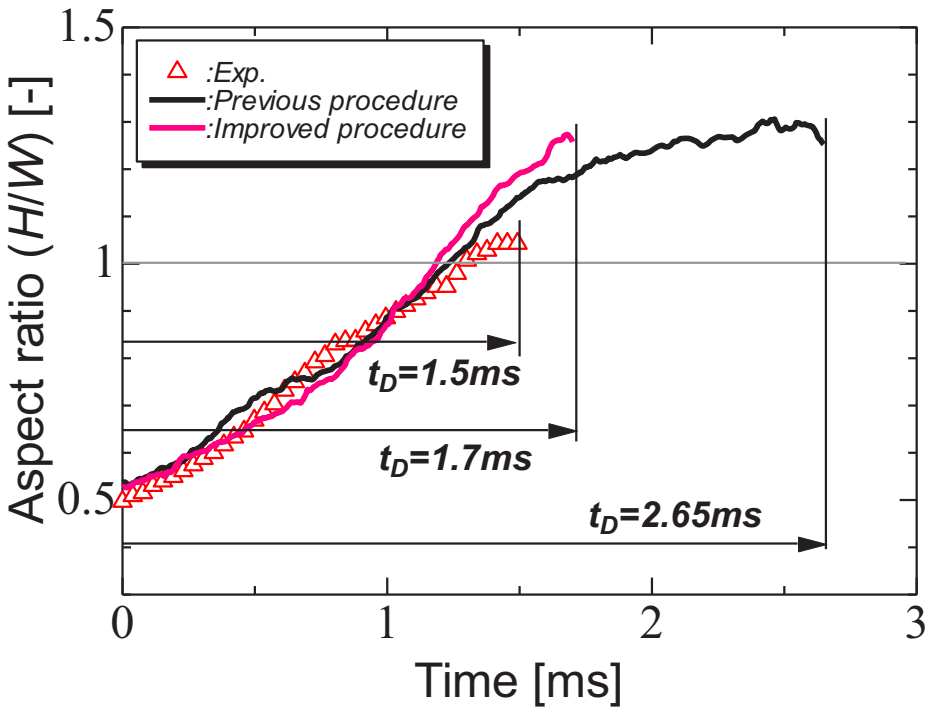

Figure 5. The comparison of bubble aspect ratio between experimental result and numerical results obtained by using both previous procedure and improved one.

4. CONCLUSIONS

In this paper, we have improved the evaluation procedure of the wall surface temperature during the subcooled nucleate boiling in the non-empirical boiling and condensation model. The improved procedure was considered the effects of microlayer evaporation for the evaluation of heat flux at the wall surface between the wall and fluid cells.

A two-dimensional axisymmetric numerical simulation of the single bubble nucleate boiling using the improved procedure was carried out, and the numerical simulation results were compared with the experimental result. The tendency of the surface temperature drop obtained from the numerical simulation based on this improvement agreed well with the experimental result.

To demonstrate the applicability of the improved procedure to the bubble-departure-period simulation at low subcooled condition, the unsteady three-dimensional numerical simulation on a single bubble departure behavior from the heating surface during the nucleate pool boiling has been conducted, and showed the good agreement for the bubble-departure-period between the numerical simulation using this improved procedure and the experiment.

ACKNOWLEDGMENTS

In this study, we thank Kyoto University to use the supercomputer of ACCMS.

REFERENCES

1. R.C. Lee and J.E. Nydahl, "Numerical calculation of bubble growth in nucleate boiling from inception through departure," *J. Heat Transfer*, **111**, pp. 474-479 (1989).
2. S.W.J. Welch, "Direct simulation of bubble growth," *Int. J. Heat and Mass Transfer*, **41**, pp. 1655-1666 (1998).
3. G. Son, V.K. Dhir and N. Ramanujapu, "Dynamics and heat transfer associated with a single bubble during nucleate boiling on a horizontal surface," *J. Heat Transfer*, **121**, pp. 623-631 (1999).
4. H.Y. Yoon, S. Koshizuka and Y. Oka, "Direct calculation of bubble growth, departure, and rise in nucleate pool boiling," *Int. J. Multiphase Flow*, **27**, pp. 277-298 (2001).
5. S. Shin, S.I. Abdel-Khalik, and D. Juric, "Direct three-dimensional numerical simulation of nucleate boiling using the level contour reconstruction method," *Int. J. Multiphase Flow*, **31**, pp. 1231-1242 (2005).
6. G. Son and V.K. Dhir, "Numerical simulation of nucleate boiling on a horizontal surface at high heat fluxes," *Int. J. Heat and Mass Transfer*, **51**, pp. 2566-2582 (2008).
7. S. Hardt and F. Wondra, "Evaporation model for interfacial flows based on a continuum-field representation of the source terms," *J. Computational Physics*, **227**, pp. 5871-5895 (2008).
8. C. Kunkelmann and P. Stephan, "CFD simulation of boiling flows using the Volume-of-Fluid method within OpenFOAM," *Numer. Heat Transfer A*, **56**, pp. 631-646 (2009).
9. C. Kunkelmann and P. Stephan, "Numerical simulation of the transient heat transfer during nucleate boiling of refrigerant HFE-7100," *Int. J. Refrigeration*, **33**, pp. 1221-1228 (2010).
10. Y. Sato and B. Ničeno, "A sharp-interface phase change model for a mass-conservative interface tracking method," *J. Computational Physics*, **249**, pp. 127-161 (2013).
11. T. Kunugi, "Brief review of latest direct numerical simulation on pool and film boiling," *Nuclear engineering and technology*, **44**(8), pp. 847-854 (2012).
12. Y. Ose and T. Kunugi, "Development of a boiling and condensation model on subcooled boiling phenomena," *Energy Procedia*, **9**, pp. 605-618 (2011).
13. T. Kunugi, "MARS for multiphase calculation," *Computational Fluid Dynamics J.*, **9**, pp. 563-571 (2001).
14. Y. Ose and T. Kunugi, "Numerical study on subcooled pool boiling," *Progress in Nuclear Science and Technology*, **2**, pp. 125-129 (2011).
15. Y. Ose and T. Kunugi, "Direct numerical simulations of subcooled boiling phenomena based on non-empirical boiling and condensation model," *Proceedings of the 15th International Heat Transfer Conference*, Kyoto, Japan, August 10-15, 2014, IHTC15-8851 (2014).
16. Y. Ose and T. Kunugi, "Numerical study on bubble behaviour and heat transfer characteristics of subcooled pool boiling based on non-empirical boiling and condensation model," *J. Computational Multiphase Flows*, **6**(4), pp. 419-429 (2014).
17. S. Jung, Y. Ose, H. Kim and T. Kunugi, "A comparison study of state-of-art experimental and numerical siluation results associated with nucleate boiling of a single bubble," *Proceedings of the 15th International Heat Transfer Conference*, Kyoto, Japan, August 10-15, 2014, IHTC15-9659 (2014).
18. J.U. Brackbill, D.B. Kothe and C. Zemach, "A continuum method for modeling surface tension," *J. Computational Physics*, **100**, pp. 335-354 (1992).
19. A. Chorin, "Numerical solution of the Navier-Stokes equations," *Mathematics of Computation*, **22**, pp. 745-762 (1968).
20. H. A. Van Der Vorst, "BI-CGSTAB: A fast and smoothly converging variant of BI-CG for the solution of nonsymmetric linear system," *SIAM Journal on Scientific and Statistical Computing*, **13**, pp. 631-644 (1992).
21. I. Ohnaka, *Introduction to computational analysis of heat transfer and solidification -application to the casting processes-*, pp. 202, Maruzen, Tokyo, Japan (1985) (in Japanese).

22. Z. Kawara, T. Okoba and T. Kunugi, “Visualization of behavior of subcooled boiling bubble with high time and space resolutions,” *Proceedings of 6th Pacific Symposium on Flow Visualization and Image Processing*, Hawaii, USA, May 16-19, 2008, pp. 424-428 (2007).